第39卷第1期
2023年1月

无 机 化 学 学 报
CHINESE JOURNAL OF INORGANIC CHEMISTRY

Vol.39 No.1
141-149

一种多吡啶双核单功能铂配合物的合成、晶体结构及抗癌活性

李训一[1,2] 王宇静[1] 周子默[1,3] 方 霄[1] 汪清清[1] 胡美纯[2] 杨晓松*[,3] 王小波*[,1]

([1]湖北科技学院医学部药学院,咸宁 437100)

([2]湖北科技学院医学部,糖尿病心脑血管病变湖北省重点实验室,咸宁 437100)

([3]湖北科技学院医学部基础医学院,咸宁 437100)

摘要: 合成了一种含有多吡啶基配体2,6-双((双(吡啶-2-基甲基)氨基)甲基)吡啶(BPA-TPA)的双核单功能铂(Ⅱ)配合物[Pt_2(BPA-TPA)Cl_2]Cl_2(**Pt_2-BPA-TPA**),以核磁共振波谱和高分辨质谱进行表征,并通过X射线单晶衍射确定了**Pt_2-BPA-TPA**的结构。琼脂凝胶电泳实验表明**Pt_2-BPA-TPA**在10 μmol·L^{-1}的低浓度下可有效切割pBR322 DNA。通过CCK-8(cell counting kit-8)实验检测了**Pt_2-BPA-TPA**对人肺癌细胞系A549的细胞毒性,结果显示**Pt_2-BPA-TPA**表现出比顺铂更好的抗癌活性,其主要通过触发DNA损伤和上调下游凋亡相关细胞信号通路蛋白(p21蛋白和cleaved-caspase-3)诱导细胞凋亡。

关键词: 单功能铂; 抗癌活性; DNA切割; 双核配合物; 晶体结构

中图分类号: O614.82+6 **文献标识码:** A **文章编号:** 1001-4861(2023)01-0141-09

DOI: 10.11862/CJIC.2022.272

Synthesis, crystal structure, and anticancer activity of a polypyridyl binuclear monofunctional platinum(Ⅱ) complex

LI Xun-Yi[1,2] WANG Yu-Jing[1] ZHOU Zi-Mo[3] FANG Xiao[1]

WANG Qing-Qing[1] HU Mei-Chun[2] YANG Xiao-Song*[,3] WANG Xiao-Bo*[,1]

([1]*School of Pharmacy, Medical Department, Hubei University of Science and Technology, Xianning, Hubei* 437100, *China*)

([2]*Hubei Key Laboratory of Diabetes and Angiopathy, Hubei University of Science and Technology, Xianning, Hubei* 437100, *China*)

([3]*School of Basic Medical Sciences, Medical Department, Hubei University of Science and Technology, Xianning, Hubei* 437100, *China*)

Abstract: A binuclear monofunctional platinum(Ⅱ) complex, [Pt_2(BPA-TPA)Cl_2]Cl_2 (**Pt_2-BPA-TPA**), containing polypyridyl ligand 2,6-bis((bis(pyridin-2-ylmethyl)amino)methyl)pyridine was synthesized and characterized by nuclear magnetic resonance and high-resolution mass spectroscopy. In addition, the structure of **Pt_2-BPA-TPA** was determined by X-ray single-crystal diffraction. Agarose gel electrophoresis experiments were used to demonstrate the efficient pBR322 DNA-cleaving activity of **Pt_2-BPA-TPA** at a low concentration of 10 μmol·L^{-1}. In CCK-8 (cell counting kit-8) cytotoxicity studies using the A549 human lung cancer cell line, **Pt_2-BPA-TPA** demonstrated enhanced anticancer activity compared with cisplatin. Mechanistic studies provided evidence that **Pt_2-BPA-TPA** induces apoptosis via triggering DNA damage and upregulating downstream cellular signaling cascades of p21 and cleaved-caspase-3. CCDC: 2115372.

Keywords: monofunctional platinum(Ⅱ); anticancer activity; DNA cleavage; binuclear complex; crystal structure

收稿日期:2022-06-28。收修改稿日期:2022-11-16。

湖北省教育厅重点项目(No.D20212802)、湖北省自然科学基金(No.2021CFB439)和湖北省卫健委项目(No.WJ2019Q022)资助。

*通信联系人。E-mail:eas7on@163.com,xiaosong_yang@hbust.edu.cn

0 Introduction

Platinum-based drugs are classic anti-cancer chemotherapeutics and are still widely used as first-line therapy to treat solid neoplasms, mainly because of their broad-spectrum anticancer activities, their distinct therapeutic effects, and their preferable economy[1-2]. Currently, approximately 50% of all chemotherapy regimens including platinum-based drugs are utilized as the main therapy or co-therapy for clinical cancer treatment[3]. Commonly used platinum-based drugs include cisplatin, carboplatin, oxaliplatin, nedaplatin, lobaplatin, and heptaplatin. All of these drugs are square-planar platinum(Ⅱ) complexes with two leaving groups and two non-leaving ligands coordinated to the Pt(Ⅱ) center[1]. Because of their structural similarity, platinum-based drugs share many general characteristics. Hence, there are indeed existing some common problems when referring to the advantages and disadvantages of platinum-based drugs. And this clinical dilemma is a serious impediment to the development of new platinum-based drugs with novel antitumor mechanisms. More unfavorably, platinum-based drugs generally demonstrate several serious side effects, including nephrotoxicity, myelosuppression, neurotoxicity, and ototoxicity, which dramatically limit their clinical use[4-7]. Another major obstacle to developing new platinum compounds with novel antitumor mechanisms is drug resistance[8-9]. It is therefore of vital importance to optimize the chemical properties, bioactivities and metabolic pathways, and mechanism of actions of novel platinum-based compounds.

Among the strategies used to overcome these adversities, one of the most common approaches is to design and exploit monofunctional platinum complexes which contain only one leaving group (in contrast with traditional platinum drugs)[10-14]. Under this principle, many monofunctional Pt complexes have been thoroughly synthesized, and their anticancer activities and mechanisms of action have been investigated[15-20]. In comparison with classical bifunctional drugs such as cisplatin, which forms bifunctional DNA adducts, monofunctional Pt complexes interact with DNA in a different manner, forming only Pt-G monoadducts[21-23]. Furthermore, most monofunctional Pt complexes undergo hydrolysis at a slower rate (than classical bifunctional Pt drugs), and they are less reactive to thiol molecules (*e. g.*, glutathione) *in vivo*, mainly due to their comparative chemical inertness and stronger hydrophobicity[24]. Conclusively, monofunctional Pt(Ⅱ) complexes bind only one strand of DNA and might target cancer without causing auditory side effects, thus having more potential development and application significance than bifunctional drugs, including cisplatin.

Considering efforts to improve the anticancer activities of platinum-based agents, the selection of non-leaving ligands is especially important when designing and preparing monofunctional platinum complexes. Groups containing nitrogen (N) donors are usually employed as leaving groups due to the thermodynamic stability of the Pt—N bonds. Thus, many monofunctional platinum complexes adopt a tridentate Pt-NNN system. For instance, Liang's group synthesized two monofunctional Pt(Ⅱ) complexes containing jatrorrhizine derivative ligands ([Pt(Jat1)Cl]Cl and [Pt(Jat2)Cl]Cl). Both of these compounds displayed remarkable anti-tumor activity on HeLa cells (with IC_{50} values of 15.01 and 1.00 $nmol \cdot L^{-1}$, respectively), and this anti-tumor activity was achieved by targeting p53 and telomerase[25]. Guo and co-workers developed a triphenylphosphonium-modified terpyridine platinum(Ⅱ) complex (TTP). TTP exhibited excellent cytotoxicity against cisplatin-insensitive human ovarian cancer cells and preferential inhibition to mitochondrial TrxR[26].

In the present study, a novel binuclear monofunctional Pt(Ⅱ) complex with a Pt-NNN coordination mode, $[Pt_2(BPA\text{-}TPA)Cl_2]Cl_2$ (**Pt_2-BPA-TPA**, BPA-TPA=2,6-bis((bis(pyridin-2-ylmethyl)amino)methyl)pyridine), was synthesized (Scheme 1). **Pt_2-BPA-TPA** was then characterized by NMR and high-resolution mass spectroscopy (HRMS). X-ray single crystal diffraction was also used to determine the structure of **Pt_2-BPA-TPA**. Thereafter, the *in vitro* DNA cleavage activity of **Pt_2-BPA-TPA** and its toxicity in the A549 cancer cell line were determined. Besides, we provided evidence for a

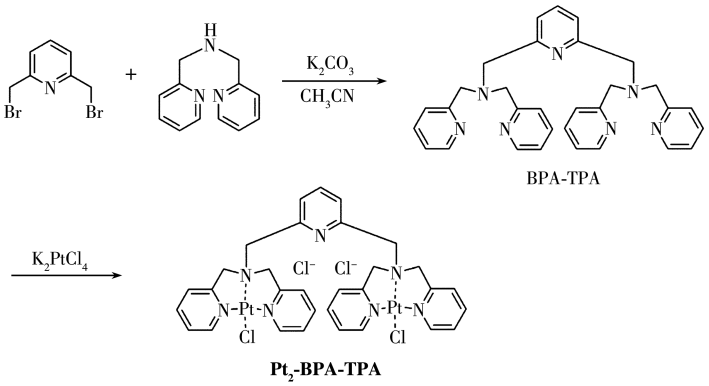

Scheme 1　Synthetic routes of ligand BPA-TPA and complex **Pt_2-BPA-TPA**

credible molecular mechanism underlying its antitumor activities. Together, our results prove that **Pt_2-BPA-TPA** is a promising candidate for novel anticancer therapy.

1　Experimental

1.1　Materials and physical measurements

All reagents were commercially obtained and, unless otherwise stated, were used without further purification. 2,6-Pyridinedimethanol was purchased from Nanjing Chemlin Co., Ltd. Bis-(2-pyridylmethyl) amine (DPA) and K_2PtCl_4 were obtained from Adamas Reagent Co., Ltd. CCK-8 (cell counting kit-8) was purchased from Dojindo Molecular Technologies Inc., Tokyo, Japan.

NMR spectra were measured on an AVANCE Ⅲ HD 400 MHz spectrometer. Electrospray ionization (ESI) mass spectra were obtained using an LCQ Fleet ThermoFisher mass spectrometer. Fluorescence spectra and UV-Vis absorption spectrum were determined on a Hitachi F-4700 fluorescence spectrometer and VARIAN CARY 50 Conc UV-visible spectrophotometer, respectively. The crystal structure of the complex was determined on a Rigaku XtaLAB PRO Ⅱ single-crystal diffractometer.

1.2　Synthesis of complex Pt_2-BPA-TPA

2,6-Bis(bromomethyl)pyridine was synthesized by previously reported methods[27]. BPA-TPA was prepared according to the reference[28]. A 2,6-bis(bromomethyl)pyridine (1.27 g, 4.8 mmol) solution, excess K_2CO_3 (1.59 g, 11.5 mmol), and DPA (1.92 g, 9.6 mmol) were added to CH_3CN under N_2 atmosphere and stirred at 30 ℃ for 2 h. After completion of the reaction, the mixture was filtered and the solvent was removed. The resulting yellow oil was extracted four times using boiling petroleum ether (b.p. 60-90 ℃) under vigorous stirring. BPA-TPA was then precipitated from the gradually cooled petroleum solution as white crystals. The purified product (2.41 g) was obtained with a yield of 56%. ^{1}H NMR (400 MHz, $CDCl_3$): δ 8.51 (d, J=4.8 Hz, 4H), 7.65-7.57 (m, 9H), 7.43 (d, J=7.7 Hz, 2H), 7.14-7.11 (m, 4H), 3.91 (s, 8H), 3.89 (s, 4H). ^{13}C NMR (100 MHz, $CDCl_3$): δ 159.32, 158.61, 149.05, 136.87, 136.45, 123.00, 122.00, 121.17, 60.20. HRMS in CH_3OH (m/z): Calcd. $[M+H]^+$ 502.272; Found: 502.322.

K_2PtCl_4 (410 mg, 1 mmol) was first dissolved in 10 mL deionized water and then mixed with 10 mL methanol containing BPA-TPA (248 mg, 0.5 mmol) in a round-bottom flask. The resulting mixture was stirred in the dark for 48 h at room temperature. A beige precipitate was collected by centrifugation, and this was carefully washed with dichloromethane, ethanol, acetone, and anhydrous ether. The purified product of Pt_2-BPA-TPA (52 mg) was obtained with a yield of 21%. ^{1}H NMR (400 MHz, DMSO-d_6): δ 8.60 (d, J=5.0 Hz, 4H), 8.20-8.16 (m, 4H), 7.74 (d, J=7.9 Hz, 4H), 7.59 (s, 3H), 7.55 (t, J=6.4 Hz, 4H), 5.40 (d, J=15.7 Hz, 4H), 5.06 (d, J=15.8 Hz, 4H), 4.26 (s, 4H). HRMS in CH_3CN (m/z): Calcd. $[M-Cl]^+$ 998.095 7; Found: 998.096 4. Calcd. $[M-2Cl]^{2+}$ 481.065 2; Found: 481.063 7. Calcd. $[M-2Cl+6H_2O]^{2+}$ 534.095 8; Found: 534.092 3.

1.3　Single-crystal structure determination

The crystal structure of **Pt_2-BPA-TPA** was deter-

mined by the single-crystal X-ray diffraction method. Whitish block single crystals were obtained upon vapor diffusion of ethyl acetate into a solution of the complex in DMSO. Data for **Pt_2-BPA-TPA** was collected on a hybrid pixel array detector (HPAD) at 293 K using graphite monochromatic Cu $K\alpha$ radiation (λ=0.154 184 nm) in the multi-scan mode. The structure was solved by direct methods using the SHELXS program of the SHELXTL package and refined using full-matrix least-squares methods with SHELXL (semi-empirical absorption corrections were applied using the SADABS program). SQUEEZE was adopted to reduce the effect originating from disordered solvent molecules. All hydrogen atoms were placed in a theoretical position. Crystal data and details of data collection and refinement for **Pt_2-BPA-TPA** are summarized in Table 1.

CCDC: 2115372.

Table 1 Crystal parameters and structure refinements for Pt_2-BPA-TPA

Parameter	**Pt_2-BPA-TPA**
Chemical formula	$C_{32}H_{37}Cl_4N_7O_2Pt_2$
Formula weight	1 083.66
Temperature / K	293
Crystal size / mm	0.06×0.05×0.04
Crystal system	Monoclinic
Space group	$P2_1/c$
a / nm	1.259 36(3)
b / nm	1.486 16(3)
c / nm	2.187 45(5)
β / (°)	105.058(2)
V / nm^3	3.953 48(16)
Z	4
D_c / (g·cm^{-3})	1.821
μ / mm^{-1}	15.832
F(000)	2 072
θ range for data collection / (°)	2.068 0-67.317 0
Index ranges (h, k, l)	$-15 \leqslant h \leqslant 14$, $-11 \leqslant k \leqslant 17$, $-26 \leqslant l \leqslant 26$
N_{ref}, N_{par}	6 885, 425
Completeness / %	98.68
Final R indices [$I>2\sigma(I)$]	R_1=0.091 7, wR_2=0.246 3
R indices (all data)	R_1=0.097 7, wR_2=0.251 1
Goodness-of-fit on F^2	1.028

1.4 DNA cleavage studies

DNA cleavage efficiency was assessed by agarose gel electrophoresis employing supercoiled pBR322 plasmid DNA. Briefly, supercoiled pBR322 plasmid DNA (200 ng) in 1×TAE buffer (Tris-HCl-EDTA) was treated with **Pt_2-BPA-TPA** or BPA-TPA (5-20 μmol·L^{-1}) in a final volume of 20 μL. All samples were incubated at 37 ℃ for 1.5 h. After treatment, loading buffer (3 μL) was added, and agarose gel electrophoresis was performed on a 1% gel (containing 1.0 μg·mL^{-1} neutral red) at 100 V for 1 h in diluted 1×TAE buffer. The gel was then visualized by photographing intercalated neutral red fluorescence under a UV illuminator. The cleavage efficiency was measured by determining the ability of the compound to excise supercoiled pBR322 DNA (SC) to its nicked circular (NC) and linear (L) forms.

1.5 CCK-8 assay

The cytotoxicity of **Pt_2-BPA-TPA** and cisplatin to human lung cancer A549 cells was measured using the CCK-8 assay. CCK-8 contains Dojindo′s highly water-soluble tetrazolium salt, 2-(2-methoxy-4-nitrophenyl)-3-(4-nitrophenyl)-5-(2,4-disulfophenyl)-2*H*-tetrazolium sodium salt (WST-8), which produces a water-soluble formazan dye upon reduction in the presence of an electron mediator. A549 cells were seeded in 96-well plates at a density of 4×10^3 cells per well and then incubated overnight. The adherent cells were then treated with different concentrations of drugs. After two days, 10 μL of the CCK-8 solution was added to each well of the plate, and the plate was incubated for 3 h in the incubator (37 ℃, φ_{CO_2}=5%). Finally, the OD_{450} value (optical density at 450 nm) was measured in a microplate reader.

1.6 Western blot analysis

A549 cells (or HepG2 cells) were homogenized in lysis buffer (#9803, CST, USA), and total protein was isolated by centrifugation at 12 000 r·min^{-1} for 15 min at 4 ℃. Total protein concentration in the lysates was quantified using a bicinchoninic acid (BCA) protein assay kit (A53225, Thermo Fisher Scientific, USA) according to the manufacturer′s instructions. The samples were then subjected to western blot analysis using

specific antibodies against α-tubulin (GB11001, ServiceBio, Wuhan, China), cleaved caspase-3 (9661S, CST, USA), and p21 (A1483, ABclonal, Wuhan, China) as described previously[29].

1.7 Statistical analysis

The data were analyzed by SPSS 19.0 software and presented as means±SD from at least three independent experiments. All the statistical results were analyzed according to the Student's *t*-test and Graphpad Prism 9.0 (GraphPad Software Inc., La Jolla, USA) was used to compare group means. A value of $p<0.05$ represented statistically significant.

2 Results and discussion

2.1 NMR and HRMS characterization of Pt_2-BPA-TPA

The structural characteristics of ligand BPA-TPA and complex **Pt_2-BPA-TPA** were elucidated by NMR and HRMS. The ^{1}H NMR spectra of **Pt_2-BPA-TPA** and BPA-TPA in DMSO-d_6 are shown in Fig.1. In comparison with the spectrum of BPA-TPA, proton signals in **Pt_2-BPA-TPA** were shifted significantly to the lower field, suggesting that Pt(Ⅱ) was coordinated to the ligand, and thus providing evidence of the formation of a binuclear Pt(Ⅱ) complex in **Pt_2-BPA-TPA**. The coordination of Pt increased steric hindrance in the two pyridyl groups, eliciting magnetic nonequivalence in the nearby methylene protons. Consequently, the H7 singlet at 3.79 was split into two doublets at 5.4 and 5.1. The existence of **Pt_2-BPA-TPA** in the CH_3CN solution was also studied with HRMS. The *m/z* peaks for [(**Pt_2-BPA-TPA**)−Cl]$^+$, [(**Pt_2-BPA-TPA**)−2Cl]$^{2+}$, and [(**Pt_2-BPA-TPA**)−2Cl+6H_2O]$^{2+}$ were observed at 998.096 4, 481.063 7, and 534.092 3, respectively. The results indicate that complex **Pt_2-BPA-TPA** is stable in CH_3CN.

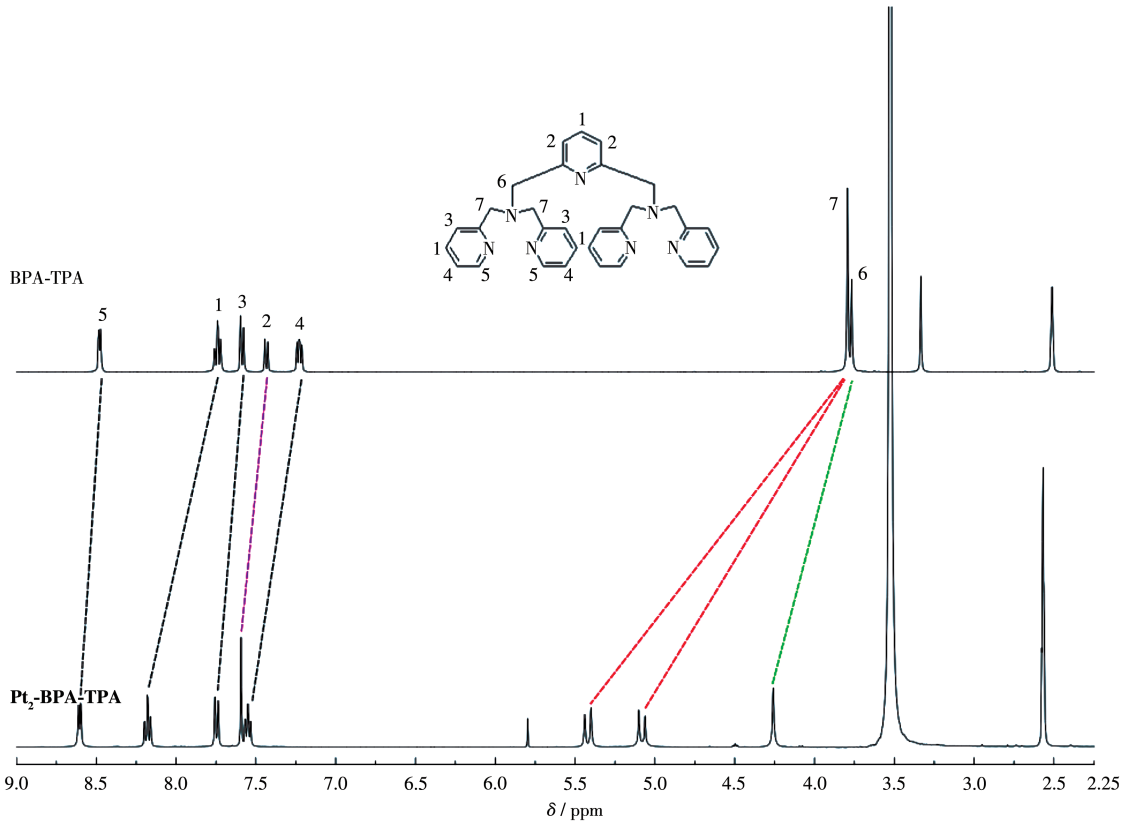

Fig.1　^{1}H NMR spectra of complex **Pt_2-BPA-TPA** and the corresponding ligand BPA-TPA

2.2 Crystal structure

As shown in Fig.2, binuclear Pt(Ⅱ) complex **Pt_2-BPA-TPA** crystallizes in a monoclinic system with space group $P2_1/c$ (centrosymmetric space group). The two Pt(Ⅱ) ions are symmetrically located in the center of the two pyridine ring arms which originate from DPA.

Each Pt(Ⅱ) ion adopts an approximate planar quadrilateral geometry associated with the [PtN_3Cl] arrangement, which is comprised of two pyridyl nitrogen atoms (for Pt1, N1 and N3; for Pt2, N4 and N6), a tertiary amine nitrogen atom (for Pt1, N2; for Pt2, N5), and a chloride atom (for Pt1, Cl1; for Pt2, Cl2). Using Pt1 as an example, the two diagonal positions are analogously occupied by N1 and N3 to yield Pt1—N1 (0.202 7(14) nm) and Pt1—N3 (0.203 9(14) nm). The dihedral angle between Cl1—Pt1—N3 and N1—Pt1—N2 is 2.166°. This dihedral angle deviates from the ideal value of 0°, implying a distorted square-planar configuration of [PtN_3Cl]. Selected bond lengths and bond angles are listed in Table 2.

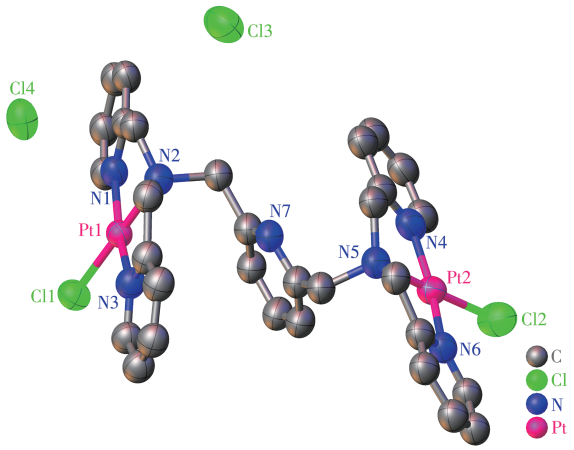

Hydrogen atoms are omitted for clarity

Fig.2 Crystal structure of **Pt_2-BPA-TPA** with 50% thermal ellipsoids

Table 2 Selected bond lengths (nm) and angles (°) for Pt_2-BPA-TPA

Pt1—Cl1	0.230 4(4)	Pt1—N1	0.202 7(14)	Pt1—N2	0.203 1(15)
Pt1—N3	0.203 9(14)	Pt2—Cl2	0.229 2(5)	Pt2—N4	0.202 0(17)
Pt2—N5	0.200 9(19)	Pt2—N6	0.204 0(14)		
Cl1—Pt1—N1	95.7(5)	Cl1—Pt1—N2	179.5(4)	Cl1—Pt1—N3	97.1(4)
N1—Pt1—N2	83.9(6)	N1—Pt1—N3	167.0(6)	N2—Pt1—N3	83.3(6)
Cl2—Pt2—N4	95.7(6)	Cl2—P2—N6	97.6(5)	Cl2—Pt2—N5	178.2(4)
N4—Pt2—N6	166.2(7)	N4—Pt2—N5	83.3(7)	N5—Pt2—N6	83.2(6)

2.3 DNA cleavage activity

The main target of platinum anticancer agents is generally believed to be nuclear DNA. The mechanism of action of Pt(Ⅱ) complexes involves the formation of Pt-DNA adducts that induce DNA damage by interfering with DNA transcription and replication, ultimately leading to cell death. To investigate the DNA cleavage activity of complex **Pt_2-BPA-TPA**, we performed agarose gel electrophoresis experiments using pBR322 plasmid DNA (1 μL, 0.2 μg) in Tris-HCl/NaCl (50 mmol·L^{-1}, pH=7.2) buffer. A significant difference in the migration rates of the three types of DNA could be observed through gel electrophoresis. The migration rates can be expected to differ as follows: supercoiled form (Form Ⅰ, SC) > linear (Form Ⅲ, L) > nicked circular (Form Ⅱ, NC)[30]. Fig.3 shows the results of gel electrophoretic separation of pBR322 plasmid DNA treated with increasing concentrations of **Pt_2-BPA-TPA**, and with the free ligand BPA-TPA. Both **Pt_2-BPA-TPA** and BPA-TPA cleaved Form Ⅰ DNA into Form Ⅱ DNA and Form Ⅲ DNA in a concentration-dependent manner. At the lowest concentration tested (5 μmol·L^{-1}), supercoiled Form Ⅰ DNA was still observed, implying the complex's weak nuclease activity at such a faint dose. Surprisingly, at 10 μmol·L^{-1} concentration, **Pt_2-BPA-TPA** and BPA-TPA exhibited efficient cleavage activity; accordingly, Form Ⅰ was

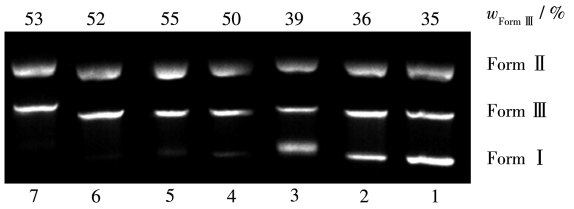

Lane 1: Control; Lane 2: DNA+BPA-TPA (5 μmol·L^{-1}); Lane 3: DNA+**Pt_2-BPA-TPA** (5 μmol·L^{-1}); Lane 4: DNA+BPA-TPA (10 μmol·L^{-1}); Lane 5: DNA+**Pt_2-BPA-TPA** (10 μmol·L^{-1}); Lane 6: DNA+BPA-TPA (20 μmol·L^{-1}); Lane 7: DNA+**Pt_2-BPA-TPA** (20 μmol·L^{-1})

Fig.3 Agarose gel electrophoresis diagrams for cleavage of pBR322 plasmid DNA induced by complex **Pt_2-BPA-TPA** and ligand BPA-TPA

relaxed to generate Form Ⅱ and Ⅲ, suggesting that double-stranded DNA was thoroughly cleaved. Under the same concentration conditions, the DNA cleavage activity of the binuclear Pt(Ⅱ) complex was not significantly higher than that of the ligand. We hypothesize that the introduction of two Pt(Ⅱ) ions does not significantly change the spatial structure of the ligand.

2.4 *In vitro* cytotoxicity

The binuclear Pt(Ⅱ) complex **Pt_2-BPA-TPA** was evaluated for its toxicity against human lung cancer A549 cells using the CCK-8 assay. Cisplatin was used as a positive control. The results are shown in Fig.4. The IC_{50} value of **Pt_2-BPA-TPA** was approximately 25 $\mu mol \cdot L^{-1}$, which was significantly lower than that of cisplatin (45 $\mu mol \cdot L^{-1}$). Therefore, **Pt_2-BPA-TPA** demonstrated increased anticancer activity on A549 cells (compared to cisplatin). As a class of non-classical platinum (Ⅱ) complexes, monofunctional platinum (Ⅱ) complexes have been widely studied to overcome the resistance and side effects of classical bifunctional platinum(Ⅱ) complexes. For instance, Guo and coworkers reported a series of mononuclear monofunctional platinum (Ⅱ) complexes with excellent anticancer activity and further investigated the anticancer mechanism[18,31-32]. Mao and coworkers developed a mononuclear monofunctional platinum(Ⅱ) complex based on lonidamine which possesses prominent cytotoxic activity against triple-negative breast cancer MDA-MB-231 cells[11]. Nevertheless, it is interesting that the binuclear monofunctional platinum(Ⅱ) complex **Pt_2-BPA-TPA** probably exhibits a new mechanism, even if its anticancer activity is modest in our present work.

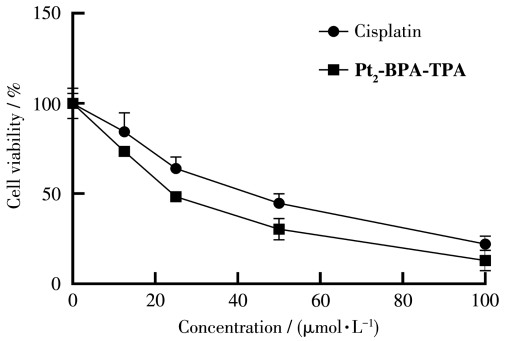

Fig.4　Dose-dependent curves showing the cytotoxicity of cisplatin and complex **Pt_2-BPA-TPA** in A549 cells

2.5 Expression of apoptosis-related proteins

Since complex **Pt_2-BPA-TPA** exhibited increased anticancer activity (compared to cisplatin), we further explored its anticancer mechanism in greater detail. p21 protein and caspase family proteins are both known to be key regulators of the apoptotic pathway. If p21 is produced in excess, the affected cell proceeds to apoptosis[33]. Caspase-3 is an important "executioner" of this apoptotic process[18,34]. To gain an insight into the molecular mechanism of cell death triggered by **Pt_2-BPA-TPA**, we used western blot assays to detect p21 and caspase-3 protein levels in HepG2, A549 cells, and rat myocardial (H9c2) cells. All three cell types were treated with **Pt_2-BPA-TPA** at concentrations of 10 or 20 $\mu mol \cdot L^{-1}$. For comparison, these

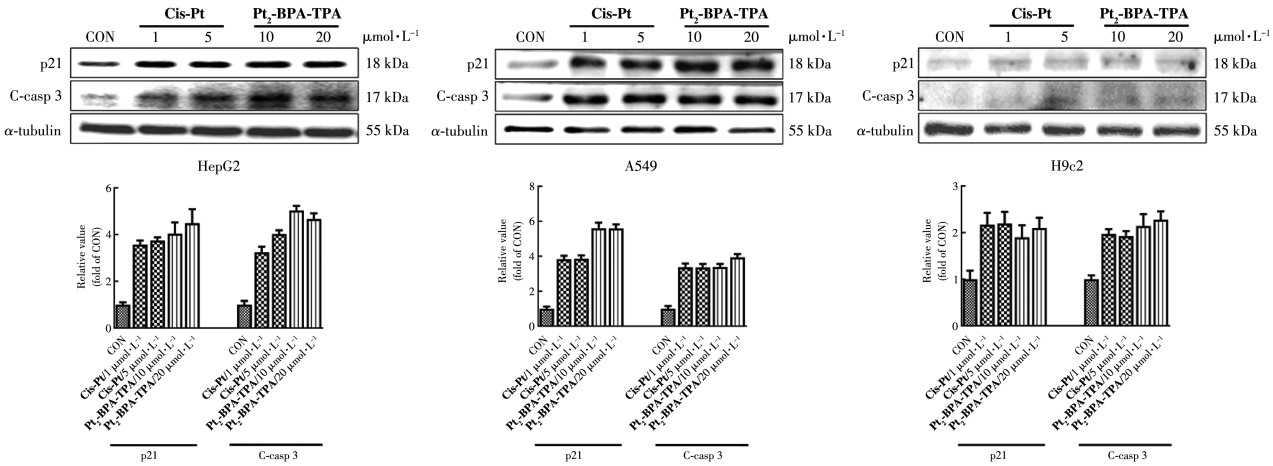

Fig.5　Expression of p21 and cleaved-caspase-3 (C-casp 3) in HepG2, A549, and H9c2 cells after incubation with cisplatin (**Cis-Pt**) and **Pt_2-BPA-TPA** for 24 h, where α-tubulin used as an internal control (CON)

cells were also treated with cisplatin at 1 and 5 μmol·L^{-1}. As shown in Fig. 5, p21 and cleaved-caspase-3 protein levels in HepG2 and A549 cells were markedly increased by **Pt_2-BPA-TPA** treatment. In A549 cells, a six-fold increase in the p21 protein level was observed, and this was significantly higher than that observed in HepG2 cells. No significant increase in either p21 protein or cleaved-caspase-3 protein levels was observed in normal H9c2 cells. These data provide solid evidence that **Pt_2-BPA-TPA** induces critical nuclear DNA damage, subsequently inducing an upregulation in the protein levels of important downstream apoptosis-related proteins, including p21 and cleaved-caspase-3.

3 Conclusions

In summary, we have successfully prepared a new binuclear monofunctional Pt(Ⅱ) complex, **Pt_2-BPA-TPA**, based on the Pt-NNN coordination pattern and employing polypyridyl as the non-leaving group. Single-crystal X-ray diffraction analysis reveals that **Pt_2-BPA-TPA** belongs to the monoclinic system with space group $P2_1/c$. The cleavage activity of **Pt_2-BPA-TPA** towards supercoiled pBR322 plasmid DNA was also studied by agarose gel electrophoresis, demonstrating that Pt_2-BPA-TPA could effectively cleave Form Ⅰ DNA to Form Ⅱ DNA and Form Ⅲ DNA. CCK-8 analysis revealed that **Pt_2-BPA-TPA** could inhibit the growth of A549 cells and that **Pt_2-BPA-TPA** demonstrated higher cytotoxicity than cisplatin after 48 h incubation. Moreover, western blot analyses provided evidence that the anticancer mechanism of **Pt_2-BPA-TPA** involves the upregulation of protein levels of important downstream apoptosis-related proteins, including p21 and cleaved-caspase-3. Generally, **Pt_2-BPA-TPA**, a refinedly synthesized binuclear monofunctional Pt(Ⅱ) complex, is a promising candidate for novel anticancer therapy.

Declaration of competing interest: All authors of this paper declare that they have no competing interests.

Acknowledgments: This project was supported by the Educational Commission of Hubei Province of China (Grant No. D20212802), the Natural Science Foundation of Hubei Province (Grant No. 2021CFB439), and the Scientific Projects of Health Commission of Hubei Province (Grant No.WJ2019Q022).

References:

[1]Yu C Q, Wang Z B, Sun Z R, Zhang L, Zhang W W, Xu Y G, Zhang J J. Platinum-based combination therapy: Molecular rationale, current clinical uses, and future perspectives. *J. Med. Chem.*, **2020**, **63**(22): 13397-13412

[2]Wheate N J, Walker S, Craig G E, Oun R. The status of platinum anticancer drugs in the clinic and in clinical trials. *Dalton Trans.*, **2010**, **39**(35):8113-8127

[3]Jin S X, Guo Y, Guo Z J, Wang X Y. Monofunctional platinum(Ⅱ) anticancer agents. *Pharmaceuticals*, **2021**,**14**:133

[4]Cheff D M, Hall M D. A drug of such damned nature. 1 Challenges and opportunities in translational platinum drug research. *J. Med. Chem.*, **2017**,**60**(11):4517-4532

[5]Kenny R G, Marmion C J. Toward multi-targeted platinum and ruthenium drugs—A new paradigm in cancer drug treatment regimens? *Chem. Rev.*, **2019**,**119**(2):1058-1137

[6]Daugaard G, Abildgaard U. Cisplatin nephrotoxicity. *Cancer Chemoth. Pharm.*, **1989**,**25**:1-9

[7]Oun R, Moussa Y E, Wheate N J. The side effects of platinum-based chemotherapy drugs: A review for chemists. *Dalton Trans.*, **2018**,**47**: 6645-6653

[8]Yimit A, Adebali O, Sancar A, Jiang Y C. Differential damage and repair of DNA-adducts induced by anti-cancer drug cisplatin across mouse organs. *Nat. Commun.*, **2019**,**10**:309

[9]Khoury A, Deo K M, Aldrich-Wright J R. Recent advances in platinum-based chemotherapeutics that exhibit inhibitory and targeted mechanisms of action. *J. Inorg. Biochem.*, **2020**,**207**:111070

[10]Sun T T, Guan X G, Zheng M., Jing X B, Xie Z G. Mitochondria-localized fluorescent BODIPY-platinum conjugate. *ACS Med. Chem. Lett.*, **2015**,**6**(4):430-433

[11]Muhammad N, Tan C P, Muhammad K, Wang J, Sadia N, Pan Z Y, Ji L N, Mao Z W. Mitochondria-targeting monofunctional platinum(Ⅱ)-lonidamine conjugates for cancer cell de-energization. *Inorg. Chem. Front.*, **2020**,**7**:4010-4019

[12]McDevitt C E, Yglesias M V, Mroz A M, Sutton E C, Yang M C, Hendon C H, DeRose V J. Monofunctional platinum(Ⅱ) compounds and nucleolar stress: Is phenanthriplatin unique? *J. Biol. Inorg. Chem.*, **2019**,**24**:899-908

[13]Imran M, Rehman Z, Hogarth G, Tocher D A, Chaudhry G S, Butler I S, Belanger-Gariepy F, Kondratyuk T. Two new monofunctional platinum(Ⅱ) dithiocarbamate complexes: Phenanthriplatin-type axial protection, equatorial-axial conformational isomerism, and anticancer and DNA binding studies. *Dalton Trans.*, **2020**,**49**:15385-15396

[14]Wu S D, Wang X Y, Zhu C C, Song Y J, Wang J, Li Y Z, Guo Z J.

Monofunctional platinum complexes containing a 4-nitrobenzo-2-oxa-1,3-diazole fluorophore: Distribution in tumour cells. *Dalton Trans.*, **2011**,**40**:10376-10382

[15]Zhou W, Almeqdadi M, Xifaras M E, Riddell I A, Yilmaz Ö H, Lippard S J. The effect of geometric isomerism on the anticancer activity of the monofunctional platinum complex *trans*-$[Pt(NH_3)_2$(phenanthridine)Cl]NO_3. *Chem. Commun.*, **2018**,**54**:2788-2791

[16]Lozada I B, Huang B, Stilgenbauer M, Beach T, Qiu Z H, Zheng Y R, Herbert D E. Monofunctional platinum(Ⅱ) anticancer complexes based on multidentate phenanthridine-containing ligand frameworks. *Dalton Trans.*, **2020**,**49**:6557-6560

[17]Zhu G Y, Myint M, Ang W H, Song L N, Lippard S J. Monofunctional platinum-DNA adducts are strong inhibitors of transcription and substrates for nucleotide excision repair in live mammalian cells. *Cancer Res.*, **2012**,**72**:790-800

[18]Guo Y, He Y F, Wu S D, Zhang S R, Song D F, Zhu Z Z, Guo Z J, Wang X Y. Enhancing cytotoxicity of a monofunctional platinum complex via a dual-DNA-damage approach. *Inorg. Chem.*, **2019**,**58**(19):13150-13160

[19]Lovejoy K S, Todd R C, Zhang S Z, McCormick M S, D'Aquino J A, Reardon J T, Sancar A, Giacomini K M, Lippard S J. *cis*-Diammine(pyridine)chloroplatinum(Ⅱ), a monofunctional platinum(Ⅱ) antitumor agent: Uptake, structure, function, and prospects. *Proc. Natl. Acad. Sci. U. S. A.*, **2008**,**105**(26):8902-8907

[20]Zhu Z Z, Wang Z H, Zhang C L, Wang Y J, Zhang H M, Gan Z J, Guo Z J, Wang X Y. Mitochondrion-targeted platinum complexes suppressing lung cancer through multiple pathways involving energy metabolism. *Chem. Sci.*, **2019**,**10**:3089-3095

[21]Johnstone T C, Wilson J J, Lippard S J. Monofunctional and higher-valent platinum anticancer agents. *Inorg. Chem.*, **2013**,**52**(21):12234-12249

[22]Chong S X, Au-Yeung S C F, To K K W. Monofunctional platinum(Pt Ⅱ) compounds—Shifting the paradigm in designing new Pt-based anticancer agents. *Curr. Med. Chem.*, **2016**,**23**(12):1268-1285

[23]Johnstone T C, Lippard S J. The chiral potential of phenanthriplatin and its influence on guanine binding. *J. Am. Chem. Soc.*, **2014**,**136**(5):2126-2134

[24]Park G Y, Wilson J J, Song Y, Lippard S J. Phenanthriplatin, a monofunctional DNA-binding platinum anticancer drug candidate with unusual potency and cellular activity profile. *Proc. Natl. Acad. Sci. U. S. A.*, **2012**,**109**(30):11987-11992

[25]Qin Q P, Zou B Q, Wang Z F, Huang X L, Zhang Y, Tan M X, Wang S L, Liang H. High *in vitro* and *in vivo* antitumor activities of luminescent platinum(Ⅱ) complexes with jatrorrhizine derivatives. *Eur. J. Med. Chem.*, **2019**,**183**:111727

[26]Wang K, Zhu C C, He Y F, Zhang Z Q, Zhou W, Muhammad N, Guo Y, Wang X Y, Guo Z J. Restraining cancer cells by dual metabolic inhibition with a mitochondrion-targeted platinum(Ⅱ) complex. *Angew. Chem. Int. Ed.*, **2019**,**58**:4638-4643

[27]Darbre T, Dubs C, Rusanov E, Stoeckli-Evans H. Syntheses of zinc complexes with multidentate nitrogen ligands: New catalysts for aldol reactions. *Eur. J. Inorg. Chem.*, **2002**(12):3284-3291

[28]Lonnon D G, Craig D C, Colbran S B, Bernhardt P V. Novel one-dimensional structures and solution behaviour of copper(Ⅱ) bromide and chloride complexes of a new pentapyridyldiamine ligand. *Dalton Trans.*, **2004**:778-787

[29]Meng X W, He C X, Chen X, Yang X S, Liu C. The extract of *Gnaphalium affine* D. Don protects against H_2O_2-induced apoptosis by targeting PI3K/AKT/GSK-3β signaling pathway in cardiomyocytes. *J. Ethnopharmacol.*, **2021**,**268**:113579

[30]Zhao J A, Yu H B, Zhi S C, Mao R N, Hu J Y, Wang X X. Synthesis, chemical nuclease activity, and *in vitro* cytotoxicity of benzimidazole-based Cu(Ⅱ)/Co(Ⅱ) complexes. *Chin. Chem. Lett.*, **2017**,**28**(7):1539-1546

[31]Xue X L, Qian C G, Fang H B, Liu H K, Yuan H, Guo Z J, Bai Y, He W J. Photoactivated lysosomal escape of a monofunctional Pt^{II} complex Pt-BDPA for nucleus access. *Angew. Chem. Int. Ed.*, **2019**,**58**(36):12661-12666

[32]Guo Y, Jin S X, Yuan H, Yang T, Wang K, Guo Z J, Wang X Y. DNA-unresponsive platinum(Ⅱ) complex induces ERS-mediated mitophagy in cancer cells. *J. Med. Chem.*, **2022**,**65**(1):520-530

[33]Westhuizen D V, Benzuidenhout D I, Munro O Q. Cancer molecular biology and strategies for the design of cytotoxic gold(Ⅰ) and gold(Ⅲ) complexes: A tutorial review. *Dalton Trans.*, **2021**,**50**:17413-17437

[34]Zhang J Z, Zhang Z L, Jiang M, Li S H, Yuan H L, Sun H B, Yang F, Liang H. Developing a novel gold(Ⅲ) agent to treat glioma based on the unique properties of apoferritin nanoparticles: Inducing lethal autophagy and apoptosis. *J. Med. Chem.*, **2020**,**63**(22):13695-13708